A smart multifunctional drug delivery nanoplatform for targeting cancer cells

Smart multifunctional drug delivery nanoplatform for targeting cancer cells

Received 00th January 20xx,
Accepted 00th January 20xx

DOI:

M. Hoop,[a] F. Mushtaq,[a] C. Hurter,[a] X.-Z. Chen,[a] B. J. Nelson,[a] and S. Pané*[a]*

Wirelessly guided magnetic nanomachines are promising vectors for targeted drug delivery, which have the potential to minimize the interaction between anticancer agents and healthy tissues. In this work, we propose a smart multifunctional drug delivery nanomachine for targeted drug delivery that incorporates a stimuli-responsive building block. The nanomachine consists of a magnetic nickel (Ni) nanotube that contains a pH-responsive chitosan hydrogel in its inner cavity. The chitosan inside the nanotube serves as a matrix that can selectively release drugs in acidic environments, such as the extracellular space of most tumors. Approximately 2.5 times higher drug release from Ni nanotubes at pH = 6 compared to pH = 7.4 is achieved. The outside of the Ni tube is coated with gold. Fluorescein isothiocyanate (FITC) labeled thiol-ssDNA, a biological marker, was conjugated on its surface by thiol-gold click chemistry, which enables traceability. The Ni nanotube allows the propulsion of the device by means of external magnetic fields. As the proposed nanoarchitecture integrates different functional building blocks, our drug delivery nanoplatform can be employed for carrying molecular drug conjugates and performing targeted combinatorial therapies, which can provide an alternative and supplementary solution to the current drug delivery technologies.

1. Introduction

In 2014, the World Health Organization (WHO) declared cancer as the major cause of deaths globally, expecting 19.3 million new diagnosed cases yearly by 2025.[1] Current cancer treatments, such as surgery, chemotherapy, and hormone therapy, cause significant undesired side effects.[2, 3] Moreover, a large variety of interconnected factors determine the efficiency of therapeutic methods.[4] Anticancer agents, which are currently administered in systemic doses, do not discriminate between cancerous and healthy tissues, causing excessive toxicity and complications in vital organs.[5] Over the two last decades, several advances have been made with anticancer therapies involving biologic and molecularly targeted agents, including drugs and monoclonal antibodies.[6-8] However, the therapeutic index of these procedures cannot be further improved due to physical and dosage constraints.[9] Furthermore, many studies report that these newly developed compounds can cause unforeseen side effects, such as cardiotoxicity, hypertension, proteinuria, and other unpredictable complications, since their interactions with other tissues are unavoidable.[10, 11] To circumvent the side effects of current and developing therapies, several intensive efforts have been made in the area of advanced functional micro- and nanomaterials for drug delivery applications.[12, 13] Many of these systems rely on accumulation in the pathological tissue or on imposed targeting moieties for active delivery.[14] Recently, the use of smart micro- and nanomachines capable of navigating through the human vasculature for drug delivery and diagnosis was proposed.[15] These structures can be precisely manipulated using different energy sources including electromagnetic fields, acoustic waves or light.[12, 16] Additionally, they can be functionalized with several chemicals, deliver drugs and cells, or capture cancer cells in complex environments.[13, 17] Incorporation of markers for device traceability in micro- and nanomachines have also been recently demonstrated.[18-20] Integrating all these features into one platform remains challenging. Furthermore, there are other aspects that must be solved such as controlling the release of the drug at the precise site or tailoring its release profile. On-demand drug release can be achieved by incorporating smart components that react in a dynamic way to abnormal cellular homeostasis such as pH, temperature or overexpressed enzymatic activities.[21] A class of smart materials is stimuli-responsive hydrogels, cross-linked polymer networks capable of hosting large amounts of small

[a] Institute of Robotics and Intelligent Systems (IRIS), ETH Zurich
Tannenstrasse 3, CH-8092 Zurich, Switzerland. E-mail: vidalp@ethz.ch, chenxian@ethz.ch

Electronic Supplementary Information (ESI) available: Fig. S1 Drug release control experiment; Fig. S2 Cell viability assay; Video – Magnetic manipulation. See DOI:

molecules (e.g. water and/or drug molecules), and allowing them to diffuse out of their networks upon changes in the physiological environment.[22-24] A major hallmark in cancer is the deregulation of the cellular energy metabolism (Warburg effect[25]), which results in an acidic microenvironment (pH ≈ 6) at the tumor due to the accumulation of the glycolytic end product lactic acid.[26, 27] These pH conditions can be used for the triggered release of drugs loaded in pH-responsive carriers, such as chitosan (Chi) hydrogels.[28, 29] Chi is a cationic polysaccharide derived from the deacetylation of chitin and consists of repeating molecules of β – (1-4) linked D-glucosamine and N-acetyl-D-glucosamine.[30, 31] The pKa value of the primary aliphatic amine group (pKa = 6.5) makes Chi insoluble at neutral/physiological conditions (pH = 7.4), but soluble and positively charged in acidic environments (pH < 6.5).[32, 33] The pH sensitivity of Chi hydrogels originates from the weak acid sensitive side chains in its polymeric backbone. Thus, altered pH values of the surrounding tissues, i.e. from physiologically healthy tissue (pH = 7.4) to neoplastic tissue (pH = 6), cause the swelling or dissolution of the hydrogel resulting in a pH-responsive drug release.[34]

In this work, we propose a versatile magnetic nanorobotic platform for smart drug delivery applications. We use template-assisted electrodeposition for the batch fabrication of magnetic nanotubes. The tubular geometry enables exo- and endofunctionalization, and, hence, high multidrug loading capacity.[35] The ferromagnetic tube serves as the propulsive block, which is actuated by means of external magnetic fields, and it carries in its inner cavity the smart drug Chi hydrogel carrier loaded with a model drug. The outside of the tube was further decorated with a Au layer for enhanced biocompatibility and for providing conjugation sites for fluorescence tags or diagnostic drugs. The current design provides a multifunctional, smart nanoscaled drug carrier for applications in cancer therapy.

2. Experimental Section

Fabrication and characterization of Ni/Chi/Au nanotubes. Electrodeposition of Ni nanotubes was conducted in commercially available polycarbonate (PC) membranes (Anodisc®) with average pore size of 2 μm. Prior to deposition, a 100 nm thick layer of Au was evaporated as a conductive working electrode by electron beam evaporation on the backside of the PC membrane. Ni tubes were electrochemically deposited with an Autolab PGSTAT302N in a three-electrode cell with platinum sheet and Ag/AgCl (with 0.1 M Na_2SO_4) as the counter and reference electrode, respectively. Ni nanotubes were fabricated at room temperature and with a constant voltage of – 1 V for 135 s from a 0.3 M Boric Acid (H_3BO_3) and 0.5 M Nickel (II) sulphate hexahydrate ($NiSO_4 \cdot 6H_2O$) plating solution with constant stirring. Chi from shrimp shells with a degree of deacetylation higher than 75% (Sigma-Aldrich) was dissolved in 1% acetic acid under overnight stirring. The solution was further filtered to remove undissolved particles. Then, the solution was diluted to 0.01 w/v % Chi with acetic acid and 5 mM Methylene Blue (MB), which was used as a model drug in later cell experiments. A PC template was attached to a glass slide and put in a beaker with the template facing up. The beaker was then filled with Chi solution and was placed in a vacuum chamber for 1 h, followed by sonication for 5 minutes. This process was repeated four times and then the template was immersed in 1M NaOH for 1 minute and placed in 10 w/v% sodium tripolyphosphate (TPP) (pH = 5) to crosslink the Chi inside the pores. Afterwards, the PC membrane was etched by chloroform. Obtained Ni/Chi nanotubes were washed in deionized (DI) water and collected with a magnet. Next, Ni/Chi nanotubes were dispersed on a Si wafer and 5 nm thick layer of Au was deposited by e-beam evaporation. Afterwards, the Ni/Chi/Au nanotubes were released by sonication.

Fluorescently labelled ssDNA (56-FAM/TTT TTC TGT CGC GCT TTT TT/3ThioMC3; idtDnA) was dissolved in Tris-EDTA buffer (Sigma Aldrich). In order to activate the thiol-functional groups, the ssDNA was incubated with 100 mM 1,4-Dithiothreitol (DTT) for 1 h. For removal of excess DTT, the activated ssDNA was placed on a NAP-5 columns (GE Healthcare) and eluted in Tris-EDTA (TE) buffer. Then 100 mM of ssDNA was added to the Ni/Chi/Au nanotubes. The tubes were incubated for 2 h.

The morphology, after each fabrication step, was investigated by SEM (Zeiss Ultra) operating at 3 kV. Furthermore, the presence of the Ni/Chi/Au in the nanotubes was investigated by energy dispersive X-ray analysis (EDX, FEI Quanta200).

Release experiments. Ni/Chi/Au nanotubes were dispersed in PBS with the concentration of 50 ppm at pH = 7.4 and pH = 6.0 and placed in the dark for 168 h (n = 5). The fluorescence of the solutions was measured at various times in a UV-vis spectrophotometer (Infinite M200 Pro, Tecan AG, Mannedorf, Switzerland) at an excitation wavelength of 660 nm and emission wavelength of 695 nm.

***In vitro* model drug release.** Human epithelial breast cancer cells (MDA-MB-231) were cultivated in cell culture medium (DMEM, 10% FCS; 100 x Antimycoticum) at physiological conditions.
For *in vitro* model drug release experiments of MB, 0.2×10^6 cells were put in a 35 mm tissue culture dish and incubated at physiological conditions for 24 h to let the cells attach to the surface. Afterwards, cells were fixed for 15 min in 4 % paraformaldehyde and transferred to PBS (pH = 6.0). Then, Ni/Chi/Au nanotubes loaded with MB were added to the samples and incubated for 24 – 48 h. Time-lapse fluorescence images were taken by epi-fluorescence inverted optical microscope (Olympus IX-81).

Cell/nanotube interaction investigated by SEM. For SEM images, cells were put on a Si chip in a 24 tissue culture well plate and incubated at physiological conditions for 24 h to let the cells attach to the surface. Afterwards, Ni/Chi/Au nanotubes were added to the cells culture and incubated for additional 8 hours. Then, cells were fixed for 15 min in 4 % paraformaldehyde. The Si chip with fixed cells was washed 3 times in DI water and placed in 1-butyl-3-methylimidazolium tetrafluoroborate for 30 s. Then, the cells were washed in a container with DI water for 30 sec and air dried, before imaging with SEM (Zeiss Ultra) operating at 3 kV.

Magnetic actuation. The Ni/Chi/Au nanotubes were manipulated by a customized magnetic actuation system (MFG-100-I, MagnetbotiX AG, Switzerland). The magnetic fields were generated by eight opposing coils (3 mT; 4 Hz). The nanotubes were dispersed in DI water, placed underneath the coil system and imaged with an integrated inverted optical microscope (Olympus IX-81).

Cell viability assay. The (3-[4,5-Dimethylthiazol-2-yl]-2,5-diphenyltetrazolium bromide (MTT) Cytotoxicity study was

conducted in 96-well plates with 1×10^4 RAW 264.7 cells in culture medium (100 μL). Cells were allowed to attach for 4 h. Then, the cell culture medium was removed and the cells were washed with PBS and exposed to different concentrations of Ni/Chi/Au nanotubes. After 24 h of incubation, the supernatant was replaced by fresh media (100 μL) and supplemented with MTT (12 mM). After 4 h of incubation, isopropanol (100 μL) and HCl (0.04 M) were added to the cells. Absorbance measurements were conducted in a microtiter plate reader (Infnite M200 Pro, Tecan AG, Mannedorf, Switzerland) at 540 nm.

3. Results and discussion

The nanodevices were fabricated by template-assisted electrodeposition of Ni tubes in polycarbonate membranes (PC), with an average pore diameter of 2 μm at a constant potential of –1 V for 135 s (Fig. 1 (i)). Then, the template was immersed in a solution containing 0.01 % Chi in 1% acetic acid and 5 mM Methylene Blue (MB) (Fig. 1 (ii)). The Chi solution was collected inside the Ni tubes by placing them in vacuum for 1 h, and the air bubbles were removed by sonication for 5 min at 50 watts. The vacuum wetting and sonication step was repeated four times to ensure complete filling of Ni nanotubes with the Chi solution. Crosslinking of the Chi was achieved by submersion in 1 M NaOH for 1 min and in tripolyphosphate (TPP) for 30 min, as previously described by Fusco et. al.[36] Afterwards, tubes were released from the template by selective etching of the PC membrane in a chloroform solution (Fig. 1 (iii)). Electron beam evaporation was used afterwards to decorate the carrier with a secondary metal layer of Au (Fig. 1 (iv)) that was further functionalized by fluorescently tagged single stranded DNA (ssDNA) (Fig. 1 (v)).

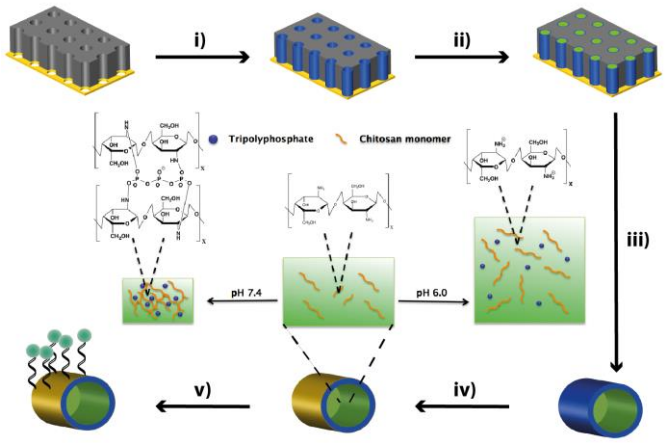

Fig. 1 Fabrication scheme. (i) Electrodeposition of Ni nanotubes in polycarbonate membranes. (ii) Filling of the nanotubes with Chi, followed by crosslinking with TPP. (iii) Release of the filled Ni/Chi tubes in chloroform. (iv) Coating Au on the outer surface of the Ni nanotube by electron-beam evaporation. (v) Functionalization of the Au surface via thiol-Au coupling. Inset: Illustration of pH responsiveness of Chi in physiological (pH 7.4) and cancerous (pH 6.0) environment is indicated.

Scanning electron microscopy (SEM) images (Fig. 2 a-c) after electrodeposition show a Ni nanotube with an average wall thickness of 200 nm, inner-diameter of 1.8 μm, and length of 6 μm. Fig. 2 d shows the filling of the tube with Chi after vacuum soaking and crosslinking. Due to deswelling of the hydrogel after vacuum drying, most of the Chi hydrogel on the inside of the tube collapsed and was pressed against the inner walls (Fig. 2 e). Energy dispersive X-ray spectrometry (EDX) maps (Fig. 2 f-j) were used in order to confirm the presence of the homogenous Ni and Au layer. Furthermore, enhanced N and C signals across the tube confirm the presence of Chi.

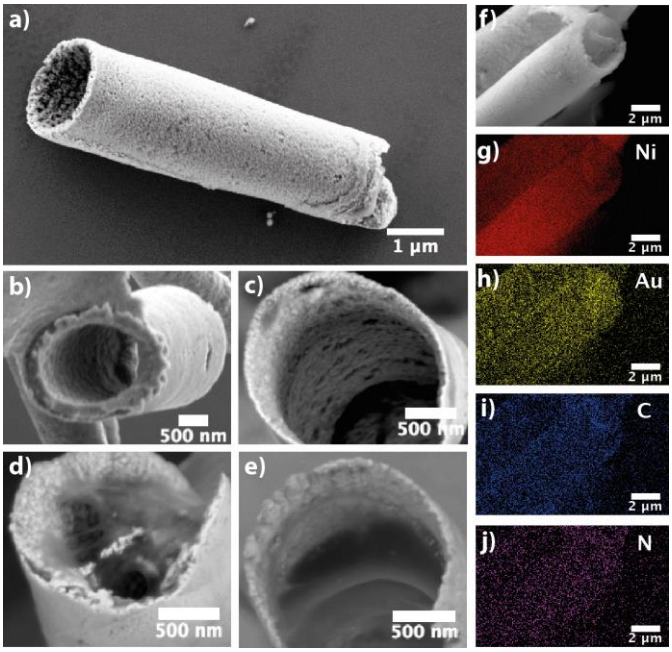

Fig. 2 SEM image of a single Ni nanotube (a). Top view SEM images, showing Ni/Au nanotubes (b-c). SEM images showing Chi inside the Ni/Au nanotubes (d-e). EDX maps of the Ni/Au/Chi nanotube (f) showing the presence of Ni (g), Au (h), C (i) and N (j).

Drug release studies from pH-responsive Chi hydrogels show significantly higher amounts of drug release at lower pH compared to physiological conditions.[36-38] To assess the ability of our nanotubes for pH triggered drug release, the Chi inside the tubes was supplemented with Methylene Blue (MB), a common model molecule for drug delivery applications, which has recently been shown to induce selectively apoptosis in cancer cells.[39, 40] The drug release efficiency of the model drug was investigated in phosphate buffered saline (PBS) solutions at pH = 6 and pH = 7.4. pH = 6 represents the average neoplastic environment and pH = 7.4 corresponds to physiological conditions in the bloodstream and healthy tissue. Fig. 3 (a) shows the drug release of Ni/Au nanotubes filled with Chi/MB at pH = 6 and 7.4. At pH = 7.4, the MB release increased within the first 24 h of incubation to 0.23 μM and remained constant afterwards. In comparison, the drug release at pH 6.0 continued to constantly increase within the initial 96 h of the experiment until it reached its equilibrium at 0.6 μM. After 48 h, the nanotubes placed in the pH = 6 solution showed significantly higher drug release (0.57 μM) than the corresponding nanotubes in physiological solution (0.23 μM). The increased MB release at pH = 6 can be attributed to the pH responsive dissolution of the Chi hydrogel due to protonated primary amine groups, which resulted in approximately 2.5 times higher drug release from Ni nanotubes at pH = 6 compared to pH = 7.4. Considering the difference in local pH between neoplastic and healthy tissue, our proposed nanotubes filled with cross-linked Chi clearly show a pH responsive drug release behavior. This is beneficial for targeted delivery of anticancer drugs at acidic tumor sites as lower amounts of therapeutic agent will be required compared to systemic

treatments. The pH responsive drug release feature, thus, will minimize the toxic side effects of anticancer drugs in vital healthy organs. A comparison study of drug release from Ni/Chi and Ni/Au/Chi nanotubes (Fig. S1) further demonstrated that the outer Au coating did not influence the drug release profile at the studied pH values.

We used breast cancer cells (MDA-MB231) to verify the pH triggered drug release of our multifunctional drug delivery systems *in vitro*. In order to simulate neoplastic *in vivo* conditions, cells were fixed and placed in a PBS solution at pH 6. Then, cells were incubated with Au coated Ni nanotubes filled with Chi/MB. Fluorescence microscopy images shown in Fig. 3 b-e, confirm the pH responsive drug release experiments. After 24 h, only a small amount of the MB was released from the drug delivery device and only cells within its direct proximity were stained. However, after 48 h, the release of MB increased and was able to affect cells at a greater distance from the structures.

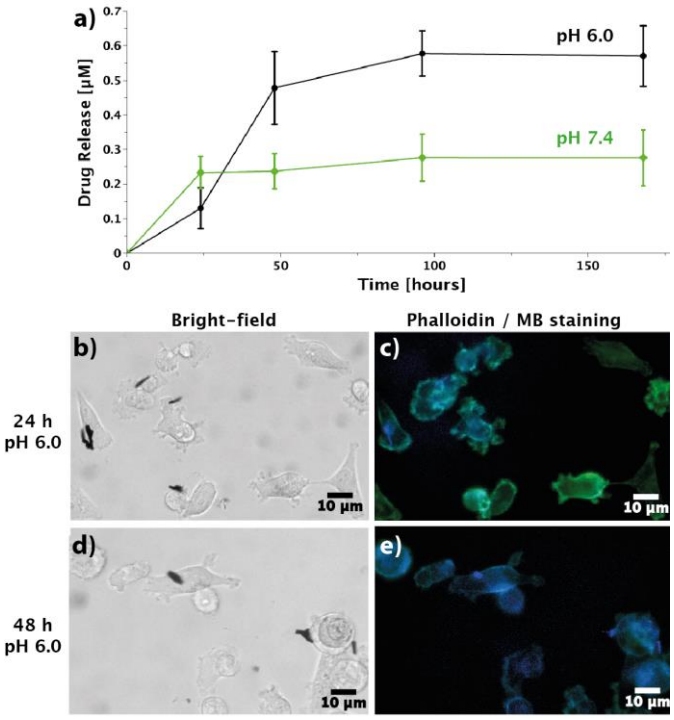

Fig. 3 Drug release profiles of MB from Ni/Au/Chi tubes at physiological (pH = 7.4) and pathological (pH = 6.0) conditions (a). *In vitro* drug delivery experiments of MB (blue) with Ni/Au/Chi nanotubes to breast cancer cells stained with phalloidin (green) at pH 6 after 24 h (b-c) and 48 h (d-e).

The cytotoxicity of Ni micro- and nanoparticles has been discussed controversially in the literature and most investigations agree that it depends on their concentration, size, shape and exposure time. For example, small nickel particles (less than 100 nm) at high concentrations show cytotoxic effects.[41-43] We tested the cytotoxic effect of Ni nanotubes coated with 5 nm of gold and filled with Chi in the concentration range of 10-100 ppm on macrophage cells by MTT assay. The results obtained in Fig. S2, confirm previous observations, where similar structures of Ni showed only low cytotoxicity.[12] Compared to previous studies on Ni nanoparticles, which were taken up by cells, in our case the Ni tubes do not undergo phagocytotic uptake by the cells, as indicated by SEM images shown in Fig. 4 a. Additionally, the gold layer on the outside further shields the Ni from the environment, possibly contributing to the low cytotoxicity.

Besides the efficiency of our multifunctional nanotubes for pH responsive drug delivery, it is imperative for biomedical applications that novel drug delivery systems can be guided to the specific target area and, furthermore, can be recovered after performing their function. In our proposed multifunctional drug delivery system, targeted locomotion is accomplished due to the ferromagnetic properties of the Ni carrier. Magnetic guidance of the nanotubes was tested by controlled propulsion experiments with uniform, low-magnitude magnetic fields.[39, 44] Here, the Au coated Ni-nanotubes filled with Chi were immersed in DI water and magnetic fields were applied. Time-lapse images shown in Fig. 4 b, demonstrate the precisely guided locomotion of the drug delivery device in a triangular trajectory (also see supplemented video).

The outer surface of the nanotubes was coated by gold in order to allow for an additional functionalization site either for tracing the device by fluorophores or conjugating a secondary drug. Multiple studies in the past have used gold surfaces for conjugation of various molecules via covalent or non-covalent interactions.[45, 46] Here, we show the successful conjugation of fluorescein isothiocyanate (FITC) labeled thiol-ssDNA via the covalent thiol-Au coupling reaction on to the outer surface of the fabricated nanotubes,[47] in order to demonstrate the fluorescence traceability of our multifunctional drug delivery device as a proof of concept. In addition, the thiol-ssDNA/FITC conjugate could also be replaced by any other drug molecule for combinatorial cancer therapy in the future. Fluorescence microscopy images in Fig. 4 c-e, illustrate the successful functionalization of the nanotubes via the thiol-ssDNA/FITC conjugate. Due to the facile thiol gold coupling, we achieved a homogenous distribution of the ssDNA/FITC molecules on the outer tube surface.

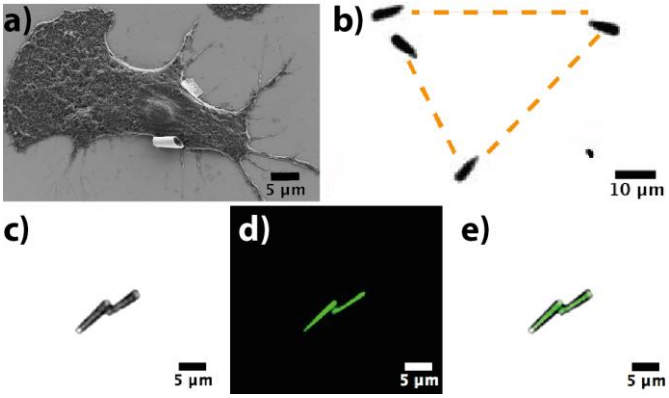

Fig. 4 (a) SEM image of breast cancer cell incubated for 24 h with Ni/Au/Chi nanotubes. (b) Controlled manipulation of the nanotubes by a magnetic field, following a triangular trajectory. (c-e) Fluorescence microscopy images of functionalized Ni/Au/Chi nanotubes with FITC tagged ssDNA.

4. Conclusion

In summary, we have designed a smart multifunctional drug delivery nanoplatform for targeting cancer cells. These nanodevices consist of magnetic nanotubes hosting in their inner cavity a smart

drug delivery building block made of pH-responsive Chi hydrogel. We demonstrate that these nanodevices show an enhanced release of drug at low pH environments such as neoplastic cell cultures. The gold-coated outer surface of the nanocarriers enables additional functionalization sites for chemical conjugation of various drug molecules, biological markers or contrast agents. [48, 49] This concept was demonstrated by attaching fluorescently tagged thiol-ssDNA on the nanotubes outer surface. Finally, the magnetic nanocarriers can be easily steered by means of external magnetic fields, thus allowing for the precise navigation of these platforms and targeted multidrug delivery applications.

Acknowledgements

We would like to acknowledge the financial support by the European Research Council Starting Grant "Magnetoelectric Chemonanorobotics for Chemical and Biomedical Applications (ELECTROCHEMBOTS)," on the ERC grant agreement no. 336456. The authors would further like to acknowledge the Scientific Center for Optical and Electron Microscopy (ScopeM) of ETH, and the FIRST laboratory for their technical support.

References

1. S. Baek, R. K. Singh, D. Khanal, K. D. Patel, E. J. Lee, K. W. Leong, W. Chrzanowski and H. W. Kim, *Nanoscale*, 2015, **7**, 14191-14216.
2. W. A. Peters, P. Y. Liu, R. J. Barrett, R. J. Stock, B. J. Monk, J. S. Berek, L. Souhami, P. Grigsby, W. Gordon and D. S. Alberts, *J. Clin. Oncol.*, 2000, **18**, 1606-1613.
3. F. S. A. M. van Dam, S. B. Schagen, M. J. Muller, W. Boogerd, E. von der Wall, M. E. D. Fortuyn and S. Rodenhuis, *J. Natl. Cancer Inst.*, 1998, **90**, 210-218.
4. A. L. Hopkins, G. M. Keseru, P. D. Leeson, D. C. Rees and C. H. Reynolds, *Nat. Rev. Drug Discov.*, 2014, **13**, 105-121.
5. K. B. Sutradhar and M. L. Amin, *ISRN Nanotechnol.*, 2014, **2014**, 1-12.
6. B. B. Aggarwal and S. Shishodia, *Biochem. Pharmacol.*, 2006, **71**, 1397-1421.
7. T. M. Allen, *Nat. Rev. Cancer*, 2002, **2**, 750-763.
8. A. B. da Rocha, R. M. Lopes and G. Schwartsmann, *Curr. Opin. Pharmacol.*, 2001, **1**, 364-369.
9. Y. Lu and R. I. Mahato, *Pharmaceutical Perspectives of Cancer Therapeutics*, Springer, Dordrecht, Heidelberg, London, New York, 2009.
10. E. Mouhayar and A. Salahudeen, *Tex. Heart Inst. J.*, 2011, **38**, 263-265.
11. A. Albini, G. Pennesi, F. Donatelli, R. Cammarota, S. De Flora and D. M. Noonan, *J. Natl. Cancer Inst.*, 2010, **102**, 14-25.
12. H. Wang and M. Pumera, *Chem. Rev.*, 2015, **115**, 8704-8735.
13. T. M. Sun, Y. S. Zhang, B. Pang, D. C. Hyun, M. X. Yang and Y. N. Xia, *Angew. Chem. Int. Ed.*, 2014, **53**, 12320-12364.
14. V. Torchilin, *Handb. Exp. Pharmacol.*, 2010, **197**, 3-53.
15. G. Tiwari, R. Tiwari, B. Sriwastawa, L. Bhati, S. Pandey, P. Pandey and S. K. Bannerjee, *Int. J. Pharm. Investig.*, 2012, **2**, 2-11.
16. S. Chowdhury, W. Jing and D. J. Cappelleri, *J. Micro-Bio Robot.*, 2015, **10**, 1-11.
17. B. J. Nelson, I. K. Kaliakatsos and J. J. Abbott, *Annu. Rev. Biomed. Eng.*, 2010, **12**, 55-85.
18. S. Ganta, H. Devalapally, A. Shahiwala and M. Amiji, *J. Control. Release*, 2008, **126**, 187-204.
19. M. Ferrari, *Nat. Rev. Cancer*, 2005, **5**, 161-171.
20. D. Peer, J. M. Karp, S. Hong, O. C. Farokhzad, R. Margalit and R. Langer, *Nat. Nanotechnol.*, 2007, **2**, 751-760.
21. S. Mura, J. Nicolas and P. Couvreur, *Nat. Mater.*, 2013, **12**, 991-1003.
22. A. Vashist, A. Vashist, Y. K. Gupta and S. Ahmad, *J. Mater. Chem. B*, 2014, **2**, 147-166.
23. G. W. Ashley, J. Henise, R. Reid and D. V. Santi, *Proc. Natl. Acad. Sci. U. S. A.*, 2013, **110**, 2318-2323.
24. M. Gonzalez-Alvarez, I. Gonzalez-Alvarez and M. Bermejo, *Ther. Deliv.*, 2013, **4**, 157-160.
25. M. G. V. Heiden, L. C. Cantley and C. B. Thompson, *Science*, 2009, **324**, 1029-1033.
26. L. Q. Chen and M. D. Pagel, *Adv. Radiol.*, 2015, **2015**, 1-25.
27. I. F. Tannock and D. Rotin, *Cancer Res.*, 1989, **49**, 4373-4384.
28. Y. Qiu and K. Park, *Adv. Drug Del. Rev.*, 2012, **64**, 49-60.
29. P. Gupta, K. Vermani and S. Garg, *Drug Discov. Today*, 2002, **7**, 569-579.
30. S. A. Agnihotri, N. N. Mallikarjuna and T. M. Aminabhavi, *J. Control. Release*, 2004, **100**, 5-28.
31. A. Popat, J. Liu, G. Q. Lu and S. Z. Qiao, *J. Mater. Chem.*, 2012, **22**, 11173-11178.
32. T. A. Sonia and C. P. Sharma, *Chitosan Biomater. I*, 2011, **243**, 23-53.
33. D. R. Bhumkar and V. B. Pokharkar, *Aaps Pharm. Sci. Tech.*, 2006, **7**, E138–E143.
34. A. Richter, G. Paschew, S. Klatt, J. Lienig, K. F. Arndt and H. J. P. Adler, *Sensors*, 2008, **8**, 561-581.
35. M. Hoop, Y. Shen, X. Z. Chen, F. Mushtaq, L. M. Iuliano, M. S. Sakar, A. Petruska, M. J. Loessner, B. J. Nelson and S. Pané, *Adv. Funct. Mater.*, 2016, **26**, 1063–1069.
36. S. Fusco, G. Chatzipirpiridis, K. M. Sivaraman, O. Ergeneman, B. J. Nelson and S. Pane, *Adv. Healthc. Mater.*, 2013, **2**, 1037-1044.
37. C. K. Chen, Q. Wang, C. H. Jones, Y. Yu, H. G. Zhang, W. C. Law, C. K. Lai, Q. H. Zeng, P. N. Prasad, B. A. Pfeifer and C. Cheng, *Langmuir*, 2014, **30**, 4111-4119.
38. R. Vivek, V. N. Babu, R. Thangam, K. S. Subramanian and S. Kannan, *Colloids Surf. B Biointerfaces*, 2013, **111**, 117-123.
39. C. Peters, M. Hoop, S. Pane, B. J. Nelson and C. Hierold, *Adv. Mater.*, 2016, **28**, 533–538.
40. G. T. Wondrak, *Free Radic. Biol. Med.*, 2007, **43**, 178-190.
41. J. R. Pietruska, X. Y. Liu, A. Smith, K. McNeil, P. Weston, A. Zhitkovich, R. Hurt and A. B. Kane, *Toxicol. Sci.*, 2011, **124**, 138-148.
42. F. Byrne, A. Prina-Mello, A. Whelan, B. M. Mohamed, A. Davies, Y. K. Gun'ko, J. M. D. Coey and Y. Volkov, *J. Magn. Magn. Mater.*, 2009, **321**, 1341-1345.
43. M. Ermolli, C. Menne, G. Pozzi, M. A. Serra and L. A. Clerici, *Toxicology*, 2001, **159**, 23-31.
44. X. Z. Chen, N. Shamsudhin, M. Hoop, R. Pieters, E. Siringil, M. S. Sakar, B. J. Nelson and S. Pané, *Mater. Horiz.*, 2016, **3**, 113-118.
45. G. Han, P. Ghosh and V. M. Rotello, *Nanomedicine*, 2007, **2**, 113-123.
46. J. P. Cheng, Y. J. Gu, S. H. Cheng and W. T. Wong, *J. Biomed. Nanotechnol.*, 2013, **9**, 1362-1369.

47. P. Ghosh, G. Han, M. De, C. K. Kim and V. M. Rotello, *Adv. Drug Del. Rev.*, 2008, **60**, 1307-1315.
48. N. L. Komarova and C. R. Boland, *Nature*, 2013, **499**, 291-292.
49. I. Bozic, J. G. Reiter, B. Allen, T. Antal, K. Chatterjee, P. Shah, Y. S. Moon, A. Yaqubie, N. Kelly, D. T. Le, E. J. Lipson, P. B. Chapman, L. A. Diaz, B. Vogelstein and M. A. Nowak, *Elife*, 2013, **2**, e00747.